LETTER

doi:10.1038/nature09617

The redox state of arc mantle using Zn/Fe systematics

Cin-Ty A. Lee[1], Peter Luffi[1], Véronique Le Roux[1], Rajdeep Dasgupta[1], Francis Albaréde[1,2] & William P. Leeman[1,3]

Many arc lavas are more oxidized than mid-ocean-ridge basalts and subduction introduces oxidized components into the mantle[1–4]. As a consequence, the sub-arc mantle wedge is widely believed to be oxidized[3,5]. The Fe oxidation state of sub-arc mantle is, however, difficult to determine directly, and debate persists as to whether this oxidation is intrinsic to the mantle source[6,7]. Here we show that Zn/Fe_T (where $Fe_T = Fe^{2+} + Fe^{3+}$) is redox-sensitive and retains a memory of the valence state of Fe in primary arc basalts and their mantle sources. During melting of mantle peridotite, Fe^{2+} and Zn behave similarly, but because Fe^{3+} is more incompatible than Fe^{2+}, melts generated in oxidized environments have low Zn/Fe_T. Primitive arc magmas have identical Zn/Fe_T to mid-ocean-ridge basalts, suggesting that primary mantle melts in arcs and ridges have similar Fe oxidation states. The constancy of Zn/Fe_T during early differentiation involving olivine requires that Fe^{3+}/Fe_T remains low in the magma. Only after progressive fractionation does Fe^{3+}/Fe_T increase and stabilize magnetite as a fractionating phase. These results suggest that subduction of oxidized crustal material may not significantly alter the redox state of the mantle wedge. Thus, the higher oxidation states of arc lavas must be in part a consequence of shallow-level differentiation processes, though such processes remain poorly understood.

Oxygen fugacity f_{O_2} is an intensive parameter describing the chemical activity of O_2 in a given system (fugacity represents a corrected partial pressure due to deviation from the ideal gas law)[8] and is used to describe the electrochemical redox potential between the different valence states of an element. Oxygen fugacity in a rock thus allows one to calculate the valence-state speciation of redox-sensitive metals, such as Fe, and of redox-sensitive species in volcanic gases[9]. In particular, f_{O_2} may have a role in the distinction between tholeiitic and calc-alkalic differentiation series, the two most voluminous magmatic differentiation series on Earth[5,10]. The calc-alkalic series is characterized by magmas for which Fe content decreases with progressive differentiation. In contrast, the tholeiitic series is characterized by magmas in which Fe progressively increases with differentiation. These differences are most probably due to a relatively oxidized redox state (high f_{O_2}, that is, greater than the f_{O_2} corresponding to the fayalite–quartz–magnetite buffer), which stabilizes Fe^{3+}-bearing oxides as fractionating phases in the calc-alkalic series and low redox state (low f_{O_2}), which suppresses Fe-oxide fractionation in the tholeiitic series[5,10,11]. Given the common association of calc-alkalic series with subduction zones and of tholeiitic series with mid-ocean-ridge environments, it is widely accepted that high f_{O_2} is a general feature of arc magmas[5]. Indeed, arc lavas are in general more oxidized than mid-ocean ridge basalts (MORBs), as evidenced[1–4] by the higher Fe^{3+}/Fe_T ratios of arc lavas (>0.1 and up to 0.5) compared to MORBs (0.1–0.2).

There is, however, no consensus on how arc magmas become more oxidized than MORBs. The prevailing view is that the high f_{O_2} of arc lavas is directly inherited from an oxidized mantle source[3]. This view is driven by the observation that much of the subducted oceanic crust appears to have been oxidized by hydrothermal seawater alteration[12]. Thus, the mantle wedge becomes oxidized upon infiltration of slab-derived fluids or melts rich in oxidized components, such as Fe^{3+} or dissolved sulphate[3,9,13], which in turn may be correlated with slab-derived water contents in arc lavas[3]. The alternative is that high f_{O_2} is not a source effect but rather the result of shallow-level differentiation processes[6,7,14], but if so, outstanding issues remain. First, to what extent can shallow-level differentiation processes, such as degassing, assimilation of oxidized materials, and fractional crystallization of reduced minerals change a magma's oxidation state after it leaves its mantle source[14]? Second, although subducted oceanic lithosphere appears to be oxidized overall[12], reduced components in the subducting slab (for example, organic-rich lithologies in hemipelagic sediments and sulphide-rich lithologies in hydrothermal systems[15]) also exist. What is their influence, if any, on arc magma compositions? Third, both oxidized and reduced lithologies are represented in sub-arc peridotites[16–20]. Does this signify a mantle wedge heterogeneous in its redox state and f_{O_2}? Finally, is the mantle's redox state buffered[21,22]? If it is buffered, for example by a C-bearing phase, or defined by a significant budget of redox-sensitive elements (for example, Fe or C species), the f_{O_2} of the mantle can only be changed by adding enough oxidized components to overwhelm the existing redox couples.

Resolving the above debate requires that we constrain the f_{O_2} of the mantle source regions of magmas, which is a difficult task. Direct approaches using the valence state of Fe or other redox-sensitive elements in whole-rocks, glasses and mineral phases reflect late equilibration conditions kinetically 'frozen' during magma cooling, and not necessarily the original melting conditions. Determining primary magmatic f_{O_2} requires us to 'see through' the effects of differentiation to retrieve past equilibrium states. Certain redox-sensitive element ratios fit this requirement[7,23]. Such ratios involve one element, the partitioning behaviour of which during mantle melting is redox-sensitive because of variable oxidation states, and another element that is not redox-sensitive because it has only one valence over the range of f_{O_2} values applicable to the mantle. Then, if the two elements of interest are incompatible in early crystallizing phases (or have similar compatibilities), their ratio will not change during magmatic differentiation, preserving a 'memory' of source f_{O_2}. For example, the ratio of redox-sensitive V to redox-insensitive Sc or Ga, that is, V_T/Sc and V_T/Ga (where V_T denotes the total concentration of V of all valences), is sensitive to the f_{O_2} during mantle melting but insensitive to early fractional crystallization because the two elements are incompatible in olivine[6,7,23]. For the most part, primitive arc basalts and MORBs have been reported to have similar V_T/Sc ratios, suggesting that MORB and arc source regions have similar f_{O_2} values[6,7]. Only arc basalts with extreme enrichments in fluid mobile trace elements show higher V_T/Sc ratios and presumably higher f_{O_2} values[7].

Independent confirmation of the above studies is desirable. Specifically, the Fe oxidation state of the primary magma should be constrained directly, because nearly all f_{O_2} constraints published so far are based on Fe valence state measurements. Recent studies of Fe isotope fractionation, which appears to be redox-sensitive, seem consistent with the V studies[24],

[1]Department of Earth Sciences, Rice University, Houston, Texas 77005, USA. [2]Ecole Normale Supérieure de Lyon, Universite Claude Bernard-Lyon I and CNRS, 69007 Lyon, France. [3]Earth Science Division, National Science Foundation, Arlington, Virginia 22230, USA.

but still require primary magmas to be measured[25]. Another approach using Fe is to examine the distribution of Fe_T/Mg between olivine and magma. Deviations of Fe_T/Mg distribution from the expected distribution of Fe^{2+}/Mg, for example:

$$K_D^{Fe^{2+}/Mg} = \frac{(Fe^{2+}_{ol}/Mg_{ol})}{(Fe^{2+}_{melt}/Mg_{melt})} \approx 0.3$$

may reflect high Fe^{3+}/Fe_T (refs 26 and 27). However, because $K_D \ll 1$, Fe_T/Mg fractionates extensively during differentiation, erasing any memory of Fe_T/Mg in the parental magma.

Here, we propose Zn/Fe_T as a redox tracer of magma sources that avoids the above limitations and complications. Over a large f_{O_2} range (from −3 log units to +4 log units relative to the fayalite–magnetite–quartz buffer: FMQ−3 to FMQ+4), Fe occurs in two valence states, Fe^{2+} and Fe^{3+} (in mantle peridotites, $Fe^{3+}/Fe_T < 0.03$) whereas Zn occurs only as Zn^{2+}. Zn and Fe^{2+} appear to behave similarly because Zn/Fe^{2+} is not fractionated significantly between olivine, orthopyroxene and basaltic melt[28], that is, $K_{D(ol/opx)}^{Zn/Fe^{2+}} \approx 1$ and $K_{D(ol/melt)}^{Zn/Fe^{2+}} = 0.8–0.9$. Because olivine and orthopyroxene account for most of the Zn and Fe in peridotites and because clinopyroxene and spinel have compensating effects (Supplementary Methods), the bulk exchange coefficient for Zn/Fe^{2+} between peridotite and melt, $K_{D(perid/melt)}^{Zn/Fe^{2+}}$, is about 1 for all pressures and temperatures relevant to mid-ocean ridge and arc magmatism. In particular, for an olivine-and-orthopyroxene-dominated peridotite, $K_{D(perid/melt)}^{Zn/Fe^{2+}}$ is largely insensitive to temperature even though individual mineral/melt partition coefficients of Zn and Fe^{2+} are temperature-dependent.

At low f_{O_2} (low Fe^{3+}/Fe_T), melting of peridotite and olivine crystallization effectively does not fractionate Zn from Fe_T. This describes the state at mid-ocean ridges, where Fe^{3+}/Fe_T is low (0.1) and MORBs and peridotites have identical Zn/Fe_T (Fig. 1). In contrast, at higher f_{O_2} (high Fe^{3+}/Fe_T), Zn/Fe_T is expected to fractionate because Fe^{3+} is incompatible in crystallizing silicate phases. For example, during partial melting of peridotite or during olivine crystallization, melts evolve towards low Zn/Fe_T. It follows that the Fe^{3+}/Fe_T of a magma can be determined from the deviations of the apparent exchange coefficient involving total Fe—that is, $K_{D(perid/melt)}^{Zn/Fe_T}$—from the true exchange coefficient $K_{D(perid/melt)}^{Zn/Fe^{2+}}$ (Fig. 2). Because peridotites have much lower Fe^{3+}/Fe_T than coexisting melts, the following equation can be derived (Supplementary Methods):

$$(Fe^{3+}/Fe_T)_{melt} \approx 1 - \frac{(Zn/Fe_T)_{melt}}{(Zn/Fe_T)_{perid}}$$

The Zn/Fe_T in peridotites can be taken as a constant ($(9.0 \pm 1) \times 10^{-4}$ by weight; Fig. 1 and ref. 28). Because it is insignificantly fractionated by

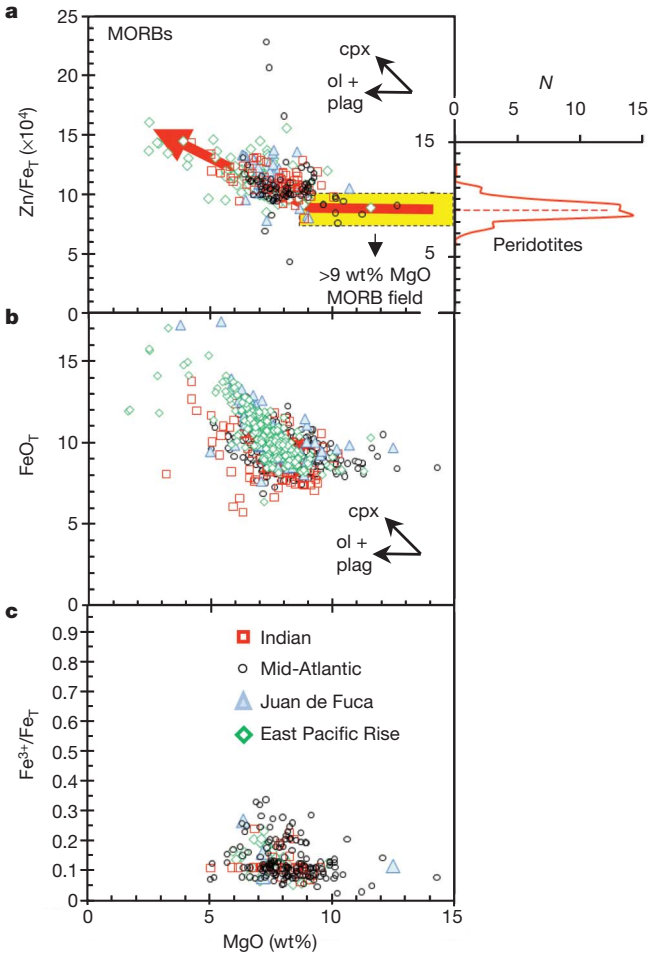

Figure 1 | Literature-compiled MORBs for different ridge systems. Data are taken from the RidgePetDB database. **a**, Zn/Fe_T ($\times 10^4$ by weight) versus MgO (wt%). The histogram on right hand axis is the distribution of peridotite xenoliths[28]. *N* is the number of peridotite samples. The dotted red line is the mean. The yellow bar represents the inferred range of Zn/Fe_T for the mantle and primary MORB. The red arrow schematically describes the trajectory over which Zn/Fe_T changes with magmatic differentiation (decreasing MgO). **b**, FeO_T versus MgO. **c**, Wet chemistry determinations of Fe^{3+}/Fe_T in whole rocks and glasses versus MgO. Small vectors correspond to olivine (ol), plagioclase (plag) and clinopyroxene (cpx) fractionation.

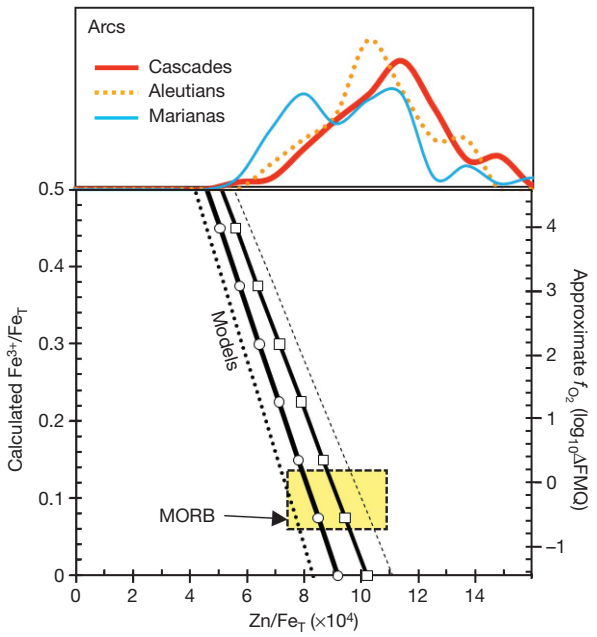

Figure 2 | Calculated Fe^{3+}/Fe_T versus Zn/Fe_T in primary basalts. The two thick black model lines were calculated using equation (1). Black line with white circles: $Zn/Fe_T = 9 \times 10^{-4}$, $K_{D(perid/melt)}^{Zn/Fe^{2+}} = 1$, $Fe^{3+}/Fe_{T(perid)} = 0.02$. Black line with white squares: $Zn/Fe_T = 9 \times 10^{-4}$, $K_{D(perid/melt)}^{Zn/Fe^{2+}} = 0.9$, $Fe^{3+}/Fe_{T(perid)} = 0.02$. The dashed thin black line is the upper bound for the model predictions: $Zn/Fe_T = 10 \times 10^{-4}$, $K_{D(perid/melt)}^{Zn/Fe^{2+}} = 0.9$, $Fe^{3+}/Fe_{T(perid)} = 0$. The dotted black line is the lower bound for the model predictions: $Zn/Fe_T = 8 \times 10^{-4}$, $K_{D(perid/melt)}^{Zn/Fe^{2+}} = 1$, $Fe^{3+}/Fe_{T(perid)} = 0.04$. The coloured curves in the top panel represent normalized histograms of Zn/Fe_T for arc lavas with MgO > 8 wt% from the Cascades ($n = 48$ for this study; $n = 136$ from the literature), the Aleutians ($n = 20$), and the Marianas ($n = 83$); see Figs 3 and 4. The yellow rectangle corresponds to the range of measured Fe^{3+}/Fe_T and Zn/Fe_T for MORBs[2]. The right vertical axis represents corresponding f_{O_2} in $\log_{10}$ unit deviations from the fayalite-magnetite-quartz buffer (FMQ) at 1 bar (f_{O_2} is approximate because it depends on melt composition and water content).

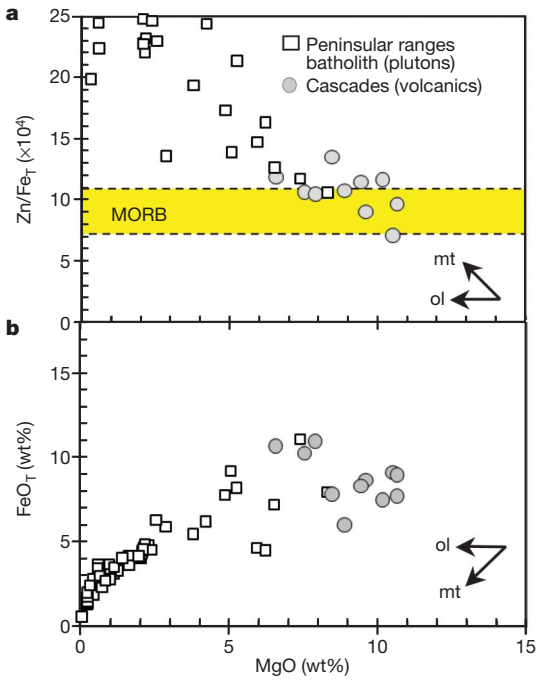

Figure 3 | Internally consistent data for a subset of primitive basalts from the Cascades arc and plutonic rocks from the Cretaceous Peninsular Ranges Batholith. Small vectors correspond to olivine (ol) and magnetite (mt) fractionation. MORB corresponds to mid-ocean basalt.

olivine removal, the Zn/Fe$_T$ of a primitive magma can then be used to estimate the Fe^{3+}/Fe$_T$ of the primary magma.

To apply this approach, we present new internally consistent Zn/Fe$_T$ data for primitive arc basalts from the Cascades volcanic arc and plutonic rocks from the Cretaceous Peninsular Ranges Batholith in southern California (Fig. 3). For comparison, we also present literature data for the Cascades along with the Marianas and Aleutian arcs (Fig. 4). Collectively, these case studies cover much of the geophysical variation in subduction zones. The Marianas island arc is associated with cold subduction, the Cascades continental arc with hot subduction, the Aleutians island arc with intermediate-aged subduction, and the Peninsular Ranges are the eroded remnants of a mature continental arc.

Plotting FeO$_T$ and Zn/Fe$_T$ against MgO (which decreases with differentiation) reveals two regimes common to the examined arc magmas, regardless of whether they are extrusive or intrusive. Zn/Fe$_T$ and FeO$_T$ remain largely constant at high MgO (regime I) until the point of magmatic differentiation, where an abrupt increase in Zn/Fe$_T$ and simultaneous decrease in FeO$_T$ (regime II) signals the onset of magnetite precipitation (Fig. 4a–f). Although the transition between the two differentiation regimes occurs at a different MgO in each arc, key conclusions can be drawn. The relatively constant Zn/Fe$_T$ and FeO$_T$ in regime I indicates that Zn and Fe$_T$ behave similarly, which implies olivine fractionation from a low-Fe^{3+}/Fe$_T$ magma, but no significant clinopyroxene or hornblende fractionation because these phases cause an increase in Zn/Fe$_T$ and FeO$_T$ given that $K_{D(cpx/melt)}^{Zn/Fe^{2+}} \approx K_{D(hb/melt)}^{Zn/Fe^{2+}} \approx 0.6$ and Fe is incompatible (Supplementary Methods). In particular, the Zn/Fe$_T$ of primitive arc magmas (MgO $>$ 8 wt%) converges to (8–11) $\times$ 10^{-4} (Figs 2–4), yielding primary Fe^{3+}/Fe$_T$ ratios

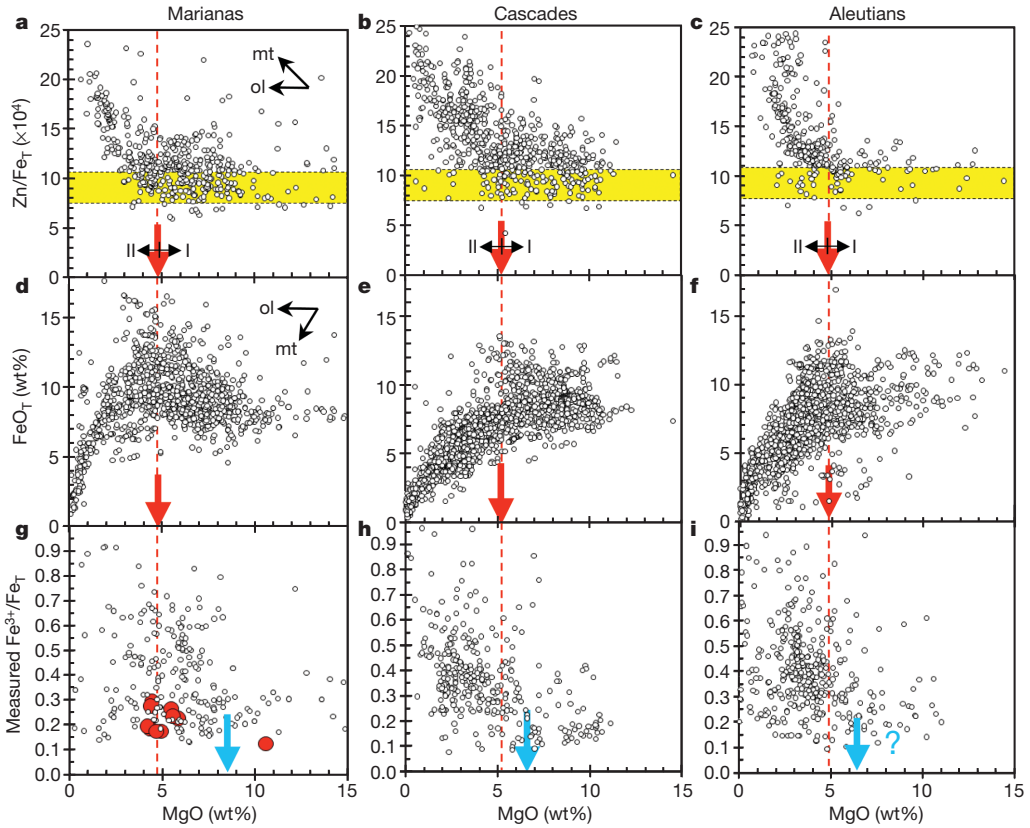

Figure 4 | Literature-compiled Zn/Fe$_T$, FeO$_T$ and wet chemistry whole-rock Fe^{3+}/Fe$_T$ versus MgO in arc lavas from the Marianas, Cascades and Aleutians. The yellow horizontal bar in **a**–**c** (the Zn/Fe$_T$ plots) corresponds to MORBs and mantle field from Fig. 1. Vertical red-dashed lines with bold red arrows mark the onset of magnetite fractionation as inferred from the onset of FeO$_T$ depletion and Zn/Fe$_T$ rise. **d**–**f**, The FeO$_T$ plots. Blue arrows in **g**–**i** (the Fe^{3+}/Fe$_T$ plots) show the MgO content at the estimated Fe^{3+}/Fe$_T$ transition from low to high. We note that the increase of Fe oxidation state commences at a higher MgO than in magnetite fractionation. Data from ref. 3 for Marianas arc melt inclusions (using their fractionation-corrected values) are also shown for reference as red-filled circles in **g**. Small vectors correspond to olivine (ol) and magnetite (mt) fractionation.

between about 0.1 and 0.15, similar to that of MORBs. Although the scatter in the data may allow for calculated Fe^{3+}/Fe_T ratios up to about 0.2–0.25, the fact that Zn/Fe_T of primitive arc magmas overlap with mantle peridotite and primitive MORBs is unequivocal (similar overlaps are seen in V_T/Sc and Mn/Fe_T; Supplementary Fig. 1). Independent of model calculations, this overlap suggests a similar overlap in Fe^{3+}/Fe_T, and implies f_{O_2} values[29] between FMQ−1 and FMQ+1, consistent with the range typical for the uppermost mantle f_{O_2} value[4,21]. If arc magmas are actually derived from peridotites more oxidized than the MORB source, the overlap between arc basalt and MORB Zn/Fe_T values would require preferential partitioning of Zn into the melt to compensate exactly for the lowering of melt Zn/Fe_T caused by melting an oxidized source. Preferential partitioning of Zn into the melt cannot be achieved by melting of harzburgitic sources because Zn/Fe_T during peridotite melting is insensitive to melting degree at pressures less than 3 GPa (ref. 28). Although partial melting of a non-peridotitic lithology, such as a garnet clinopyroxenite, with bulk $K_{D(rock/melt)} < 1$ (ref. 28), could result in elevated magmatic Zn/Fe_T, there is no evidence so far that pyroxenites are a dominant lithology in the mantle wedge.

The increasing magmatic Zn/Fe_T values in regime II require Zn to fractionate strongly from Fe_T. The onset of such fractionation is plausibly explained by Fe^{3+} becoming compatible in the fractionating minerals while Zn and Fe^{2+} remain moderately incompatible. Magnetite and hornblende are the only phases that are likely to cause simultaneous decrease in Fe_T and increase in Zn/Fe_T. Their formation implies an increase in magmatic Fe^{3+}/Fe_T to levels sufficient to saturate Fe^{3+}-bearing minerals as fractionating phases. This inference is supported by literature-compiled wet chemistry measurements of Fe^{3+}/Fe_T in whole rocks and glasses in Fig. 4g–i (see Supplementary Methods for discussion of data quality). Much of the variability in Fe^{3+}/Fe_T may be due to post-eruptive oxidation processes, such as weathering and alteration, so it is likely that measured Fe^{3+}/Fe_T ratios represent maximum bounds. However, a common feature of all the examined arcs is that measured Fe^{3+}/Fe_T is low in primitive (high MgO) lavas and that the average Fe^{3+}/Fe_T and also its variability increase markedly as MgO decreases. Thus, both measured values and those inferred from Zn/Fe_T for Fe^{3+}/Fe_T increase with progressive magmatic differentiation. We also note that, during magmatic differentiation, the increase in Fe^{3+}/Fe_T precedes (occurs at a higher MgO) the increase in Zn/Fe_T and decrease in FeO_T (where FeO_T is total Fe taken as FeO), consistent with the above suggestion that saturation of Fe^{3+}-bearing oxides (or Fe^{3+}-bearing silicates, such as amphibole), occur only after f_{O_2} and Fe^{3+}/Fe_T of the magma increase to sufficient levels.

Our results suggest that, on average, the f_{O_2} of the uppermost mantle is relatively constant. Thus, subduction of oceanic lithosphere does not systematically oxidize the mantle wedge beneath arcs. Two possibilities are: (1) subducting oceanic lithosphere and sediments are not oxidized in total or (2) the oceanic lithosphere is oxidized but the oxidized components are retained during slab melting or dehydration. A more likely explanation, however, is that the input of oxidized components from the slab into the mantle wedge is not high enough to overwhelm the redox-buffering capacity of the upper mantle. For example, the concentration of buffering phases (such as elemental carbon, carbonate or sulphide) or bulk Fe may be sufficiently elevated in the mantle that its redox state is resistant to perturbations. The abundances of carbon and sulphur in the mantle need to be better constrained to evaluate this suggestion[22]. In any case, we do not rule out the possibility of locally oxidized regions in the mantle wedge or lithospheric mantle associated with metasomatism. Indeed, the most oxidized magmas tend to be high-potassium types (for example, shoshonites and minettes), which may originate by partial melting of metasomatic veins in the mantle[30].

The above observations lead us to predict that arc magmas oxidize during differentiation. One possibility is that because Fe^{3+} is excluded from early crystallizing silicates, such as olivine, Fe^{3+}/Fe_T increases in the magma with progressive olivine fractionation (a 50% crystallization of olivine doubles the Fe^{3+}/Fe_T of the magma). However, olivine fractionation alone provides no explanation for the distinction between calc-alkalic and tholeiitic differentiation series. An alternative contributing factor may be auto-oxidation processes involving degassing. It has been suggested that magmatic Fe^{3+}/Fe_T may increase owing to the formation of micro-crystalline magnetite by reaction of water with ferrous oxide species in the melt and release of H_2 (ref. 31), but the significance of this effect in arcs is not clear. Any successful alternative to the 'source' hypothesis for the oxidation state of arc magmas must explain the observed correlation between high oxidation state and water content in arc lavas[3].

METHODS SUMMARY

Zn/Fe^{2+} exchange coefficients between olivine, orthopyroxene, clinopyroxene and spinel were inferred from the Zn/Fe ratios of minerals in natural peridotites[28]. Bulk peridotite/melt exchange coefficients were inferred by (1) assuming primitive MORB is in equilibrium with peridotite, and (2) tracking Zn/Fe in peridotites as a function of melting degree[28]. Collectively, these data were used to estimate mineral/melt exchange coefficients. Zn/Fe_T data presented for natural samples were compiled from the literature or represent new, solution-based inductively coupled plasma mass spectrometry analyses. Fe^{3+}/Fe_T data represent wet chemistry results of whole-rock data compiled from the literature (following filtering schemes presented in the Supplementary Methods).

Received 10 May; accepted 19 October 2010.

1. Carmichael, I. S. E. The redox states of basic and silicic magmas: a reflection of their source regions? *Contrib. Mineral. Petrol.* **106,** 129–141 (1991).
2. Bezos, A. & Humler, E. The Fe^{3+}/Fe ratios of MORB glasses and their implications for mantle melting. *Geochim. Cosmochim. Acta* **69,** 711–725 (2005).
3. Kelley, K. A. & Cottrell, E. Water and the oxidation state of subduction zone magmas. *Science* **325,** 605–607 (2009).
4. Christie, D. M., Carmichael, I. S. E. & Langmuir, C. H. Oxidation states of mid-ocean ridge basalt glasses. *Earth Planet. Sci. Lett.* **79,** 397–411 (1986).
5. Gill, J. B. *Orogenic Andesites and Plate Tectonics* (Springer, 1981).
6. Mallmann, G. & O'Neill, H. S. C. The crystal/melt partitioning of V during mantle melting as a function of oxygen fugacity compared with some other elements (Al, P, Ca, Sc, Ti, Cr, Fe, Ga, Y, Zr and Nb). *J. Petrol.* **50,** 1765–1794 (2009).
7. Lee, C.-T. A., Leeman, W. P., Canil, D. & Li, Z.-X. A. Similar V/Sc systematics in MORB and arc basalts: implications for the oxygen fugacities of their mantle source regions. *J. Petrol.* **46,** 2313–2336 (2005).
8. Frost, B. R. in *Oxide Minerals: Petrologic and Magnetic Significance* (ed. Lindsley, D. H.) Vol. 25, 1–9 (Mineral. Soc. Am. Rev. Min., 1991).
9. Wood, B. J., Bryndzia, L. T. & Johnson, K. E. Mantle oxidation state and its relationship to tectonic environment and fluid speciation. *Science* **248,** 337–345 (1990).
10. Osborn, E. F. Role of oxygen partial pressure in the crystallization and differentiation of basaltic magma. *Am. J. Sci.* **257,** 609–647 (1959).
11. Arculus, R. J. Use and abuse of the terms calcalkaline and calcalkalic. *J. Petrol.* **44,** 929–935 (2003).
12. Alt, J. C., Honnorez, J., Laverne, C. & Emmermann, R. Hydrothermal alteration of a 1 km section through the upper oceanic crust, Deep Sea Drilling Project Hole 504B: mineralogy, chemistry, and evolution of seawater-basalt interactions. *J. Geophys. Res.* **91,** 10309–10335 (1986).
13. Mungall, J. E. Roasting the mantle: slab melting and the genesis of major Au and Au-rich Cu deposits. *Geology* **30,** 915–918 (2002).
14. Sisson, T. W. & Grove, T. L. Experimental investigations of the role of H_2O in calc-alkaline differentiation and subduction zone magmatism. *Contrib. Mineral. Petrol.* **113,** 143–166 (1993).
15. Patino, L. C., Carr, M. J. & Feigenson, M. D. Local and regional variations in Central American arc lavas controlled by variations in subducted sediment input. *Contrib. Mineral. Petrol.* **138,** 265–283 (2000).
16. McInnes, B. I. A., Gregoire, M., Binns, R. A., Herzig, P. M. & Hannington, M. D. Hydrous metasomatism of oceanic sub-arc mantle, Lihir, Papua New Guinea: petrology and geochemistry of fluid-metasomatised mantle wedge xenoliths. *Earth Planet. Sci. Lett.* **188,** 169–183 (2001).
17. Parkinson, I. J. & Arculus, R. J. The redox state of subduction zones: insights from arc-peridotites. *Chem. Geol.* **160,** 409–423 (1999).
18. Ishimaru, S., Arai, S. & Shukuno, H. Metal-saturated peridotite in the mantle wedge inferred from metal-bearing peridotite xenoliths from Avacha volcano, Kamchatka. *Earth Planet. Sci. Lett.* **284,** 352–360 (2009).
19. Malaspina, N., Poli, S. & Fumagalli, P. The oxidation state of metasomatized mantle wedge: insights from C-O-H-bearing garnet peridotite. *J. Petrol.* **50,** 1533–1552 (2009).
20. Wang, J., Hattori, K. H., Kilian, R. & Stern, C. R. Metasomatism of sub-arc mantle peridotites below southernmost South America: reduction of fO_2 by slab-melt. *Contrib. Mineral. Petrol.* **153,** 607–624 (2007).
21. Frost, D. J. & McCammon, C. A. The redox state of Earth's mantle. *Annu. Rev. Earth Planet. Sci.* **36,** 389–420 (2008).
22. Canil, D. *et al.* Ferric iron in peridotites and mantle oxidation states. *Earth Planet. Sci. Lett.* **123,** 205–220 (1994).

23. Canil, D. Vanadium partitioning and the oxidation state of Archaean komatiite magmas. *Nature* **389,** 842–845 (1997).
24. Dauphas, N. *et al.* Iron isotopes may reveal the redox conditions of mantle melting from Archean to present. *Earth Planet. Sci. Lett.* **288,** 255–267 (2009).
25. Teng, F.-Z., Dauphas, N. & Helz, R. T. Iron isotope fractionation during magmatic differentiation in Kilauea Iki lava lake. *Science* **320,** 1620–1622 (2008).
26. Roeder, P. L. & Emslie, R. F. Olivine-liquid equilibrium. *Contrib. Mineral. Petrol.* **29,** 275–289 (1970).
27. Lange, R. A. & Carmichael, I. S. E. The Aurora volcanic field, California-Nevada: oxygen fugacity constraints on the development of andesitic magma. *Contrib. Mineral. Petrol.* **125,** 167–185 (1996).
28. Le Roux, V., Lee, C.-T. A. & Turner, S. J. Zn/Fe systematics in mafic and ultramafic systems: implications for detecting major element heterogeneities in the Earth's mantle. *Geochim. Cosmochim. Acta* **74,** 2779–2796 (2010).
29. Kress, V. C. & Carmichael, I. S. E. The compressibility of silicate liquids containing Fe_2O_3 and the effect of composition, temperature, oxygen fugacity and pressure on their redox states. *Contrib. Mineral. Petrol.* **108,** 82–92 (1991).
30. Rowe, M. C., Kent, A. J. R. & Nielsen, R. L. Subduction influence on oxygen fugacity and trace and volatile elements in basalts across the Cascade Volcanic Arc. *J. Petrol.* **50,** 61–91 (2009).
31. Holloway, J. R. Redox reactions in seafloor basalts: possible insights into silicic hydrothermal systems. *Chem. Geol.* **210,** 225–230 (2004).

Supplementary Information is linked to the online version of the paper at www.nature.com/nature.

Acknowledgements Discussions and debates with D. Canil, R. Lange, E. Cottrell and K. Kelley are appreciated. We especially thank H. O'Neill for insights. This work was facilitated by a Geological Society of America award (to C.-T.A.L.) F.A. was supported by the Keith-Weiss Visiting Professorship at Rice University.

Author Contributions C.-T.A.L. designed the project and wrote the paper, P.L. compiled the ferric iron contents of arc lavas, measurements were done by C.-T.A.L. and V.L.R., and all authors contributed to discussions and data analysis.

Author Information Reprints and permissions information is available at www.nature.com/reprints. The authors declare no competing financial interests. Readers are welcome to comment on the online version of this article at www.nature.com/nature. Correspondence and requests for materials should be addressed to C.-T.A.L. (ctlee@rice.edu).